

# Fatigue crack-propagation in annealed poly(butylene terephthalate)

J. T. YEH, J. RUNT\*

*Polymer Science Program, Department of Materials Science and Engineering,  
The Pennsylvania State University, University Park, Pennsylvania 16802, USA*

Samples with the same percentage crystallinity, supermolecular structure and lamellar thickness but different average molecular weight were prepared to distinguish the effect of tie chain density on fatigue crack propagation (FCP) behaviour. This alteration in molecular weight was accomplished by "controlled" chain degradation during thermal annealing. A significant decrease in FCP resistance was observed when samples were annealed at different temperatures for various amounts of time. In addition, an examination of the fracture surfaces of these specimens indicates a transition to a more brittle-type behaviour when annealed for longer periods of time at any specific annealing temperature. The decrease in FCP resistance is attributed to a decrease in the tie chain density.

## 1. Introduction

The dynamic fatigue behaviour of both amorphous and semicrystalline polymers has been actively investigated for many years [1, 2]. Despite the relatively large body of work on fatigue resistance of semi-crystalline polymers, relatively few studies concerning the effect of crystalline morphology (i.e. degree of crystallinity ( $W_c$ ), tie molecule density ( $f_T$ ), spherulite size ( $D$ ) and lamellae thickness ( $L$ ) on fatigue have been conducted [3-7]. By focusing on these few publications, results concerning the influence of the degree of crystallinity and spherulite size on fatigue crack propagation (FCP) resistance seem to be more conclusive and draw more attention than the effect of  $f_T$ . This is probably because of the relative ease of measuring  $W_c$  and  $D$  and the difficulty in estimating  $f_T$  for a significant number of bulk specimens. For example, a striking effect of  $W_c$  on FCP rates of high density polyethylene (HDPE) has been demonstrated by de Charentenay and co-workers [3]. They reported that FCP rates in HDPE decreased by about an order of magnitude as crystallinity increased by about 8 to 9% in samples with a weight average molecular weight of about  $70\,000\text{ g mol}^{-1}$ . Recently, more evidence supporting the beneficial effect of  $W_c$  on FCP rates has been reported by Ramirez *et al.* [4]. In that publication, amorphous poly(ethylene terephthalate) (PET) was reported to exhibit unusually high FCP resistance in contrast to other amorphous polymers. This exceptional fatigue resistance was attributed to the development of crystallinity at the crack tip during the fatigue test. The influence of spherulite size and distribution has probably been best demonstrated by Friedrich [5]. He concluded that the FCP resistance of isotactic polypropylene decreased with increasing content of large spherulites.

However, in contrast to the effects of  $W_c$  and  $D$ , the influence of the tie chain density has attracted little attention. More recently, evidence supporting the influence of tie chain density on FCP behaviour of PET was reported by Ramirez *et al.* [6]. In that publication, variation in  $W_c$ , crystal size and/or crystal perfection was obtained by annealing amorphous PET at four different temperatures for various amounts of time. At any annealing temperature, at a constant value of the stress intensity factor range ( $\Delta K$ ), FCP rates first increase slightly, then decrease as annealing proceeds, and then increase catastrophically. The reason for the initial increase in FCP rate with increasing crystallinity is still not clearly understood. The decrease in FCP rate with increasing  $W_c$  has been explained as reflecting the corresponding increase in the ability to dissipate energy through the crystallite deformation. However, at an even higher  $W_c$ , the authors postulated that tie chain density decreases to a point where no effective entanglement network is formed to link the crystallites, and fracture readily occurs. In a recent investigation [7], we drew a similar conclusion concerning the competing effects of  $f_T$  and  $W_c$  on a slightly branched polyethylene. In this study, as well as in the present investigation, tie molecule density was followed using an indirect method.

Based on the results presented so far, strictly speaking, the effects of the spherulite size, crystalline content and/or lamellae thickness on FCP behaviour of semicrystalline polymers have never been successfully differentiated from that of tie chain density. One of the reasons for this is probably the difficulty of varying the tie molecule density independently. One way of doing this is by causing chain scission in the amorphous phase while leaving the crystalline phase essentially unmodified. This may be achieved through carefully

\*To whom correspondence should be addressed.

annealing a polymer which is susceptible to degradation at elevated temperatures. For example, polybutylene terephthalate (PBT) is well known to be susceptible to chain degradation (e.g. hydrolysis). In the present study, specimens with the same degree of crystallinity, supermolecular structure and lamellae thickness but different tie chain densities, were prepared by annealing quenched PBT samples at three temperatures for various periods of time. The influence of  $f_T$  has been isolated and found to exhibit a dramatic influence on the FCP resistance.

## 2. Experimental procedure

### 2.1. Sample preparation

Injection-moulded PBT (Celanex 2000, without stabilizer) plaques were obtained from Hoechst-Celanese. The plaques were then machined into compact-tension specimens with dimensions of  $2.45'' \times 2.3'' \times 0.125''$  (1 inch = 2.54 cm) thick. Before sample preparation, these plaques were dried in a vacuum oven at  $110^\circ\text{C}$  for 16 h. The dried plaques were initially melted in a silicone oil bath at  $255^\circ\text{C}$  for 10 min and then quickly quenched into ice water. The quenched samples were maintained at room temperature overnight in a vacuum desiccator. Samples were then annealed for varying amounts of time at temperatures ranging from  $130$  to  $200^\circ\text{C}$ . After the required annealing, the samples were air cooled.

### 2.2. Fatigue crack propagation experiments

All fatigue experiments were performed on a computer controlled 1331 Instron servohydraulic test system, using a sinusoidal waveform, a minimum-to-maximum load ratio ( $R$ ) of 0.1 and a frequency of 1 Hz. A GE video camera and a Panasonic video cassette recorder were used to monitor crack length. The prepared plaques were initially notched with a hacksaw and then sharpened with a scalpel blade. The initial crack length was about 2.1 cm. No crack growth data were taken until the crack had grown several millimetres past the precracked zone.

The stress intensity factor ( $K$ ) for the compact tension specimen was calculated [8] from the applied load ( $P$ ), the specimen thickness ( $B$ ), the distance from the pin loading axis to the back edge of the specimen ( $W$ ), and a geometrical factor  $f(a/W)$

$$K = [P/(BW^{1/2})] \times f(a/W) \quad (1)$$

where

$$f(a/W) = \{[2 + (a/W)]/[1 - (a/W)]\}^{3/2} \times [0.886 + 4.64(a/W) - 13.32(a/W)^2 + 14.72(a/W)^3 - 5.6(a/W)^4]$$

and  $a$  is the crack length. Plots of  $da/dN$  (the crack propagation rate) against  $\Delta K$  are used to compare the fatigue behaviour obtained from different samples.

## 2.3. Characterization

### 2.3.1. Intrinsic viscosity

Since PBT is well known to be susceptible to molecular weight degradation (eg. by hydrolysis [9]), intrinsic viscosity measurements were conducted on the various

samples in order to establish any possible effect of the annealing treatment on the molecular weight of the polymer. The intrinsic viscosities ( $[\eta]$ ) of the prepared plaques were determined using a Cannon-Ubbelohde viscometer at  $25^\circ\text{C}$  in a phenol/tetrachloroethane mixture (60:40 weight). The number average molecular weight ( $M_n$ ) was determined by applying the expression reported by Devaux *et al.* [10]

$$[\eta] = 2.15 \times 10^{-4} \times M_n^{0.82} (\text{dl g}^{-1}) \quad (2)$$

### 2.3.2. Degree of crystallinity and lamellar thickness

The melting behaviour and the degree of crystallinity of all samples were studied by using a Perkin-Elmer differential scanning calorimeter model 7. Baselines used in the experiments were adjusted to have a maximum fluctuation of less than 0.1 mW over the temperatures range of interest. The degrees of crystallinity at room temperature of all samples were calculated using baselines drawn from  $130$  to  $270^\circ\text{C}$  and a perfect crystal heat of fusion of  $142 \text{ J g}^{-1}$  [11]. Typical sample weight used in the DSC experiments was 5 mg for  $W_c$  measurement and 0.5 mg for  $T_m$  measurement. Scans were carried out under flowing argon at a heating rate of  $20^\circ\text{C min}^{-1}$ . The instrument was calibrated using pure indium.

Lamellae thickness was not directly measured directly but estimated from the observed melting temperature ( $T_m$ ) by using the Hoffman-Weeks equation [12]. A value of  $0.036 \text{ J m}^{-2}$  for the end surface free energy and  $250^\circ\text{C}$  for the equilibrium melting temperature were used in our calculation. These values were obtained based on the results presented by Fakirov *et al.* [13]. The second melting peaks at about  $221^\circ\text{C}$  were chosen, as a first approximation, to represent the melting of the as-formed crystals.

### 2.3.3. Supermolecular structure and size

Supermolecular structure was viewed through crossed polarizers with an Olympus BHSP-300 optical microscope equipped with a PM-10AD photomicrographic system.  $2 \mu\text{m}$  thick sections were cut from test pieces of bulk polymer using a Reichert-Jung Ultracut E Microtome equipped with a glass knife at room temperature. In addition, we also attempted to use small angle laser light scattering (SALS) to evaluate the supermolecular structure. The light scattering was conducted under crossed polars (Hv scattering) using a model 1460 optical multichannel analyser, equipped with a two-dimensional position sensitive vidicon detector. The source was a 4 mW, He-Ne gas laser ( $\lambda = 632.8 \text{ nm}$ ).

### 2.3.4. Tie molecule density

Tie molecule density was not measured directly but evaluated from brittle tensile strength measurements as suggested by Brown and Ward [14]. We are not suggesting that these evaluations provide a precise measurement of the tie chain density but rather, qualitative information which will allow a comparison of various samples for a given polymer. The brittle tensile strength of dogbone-shaped specimens were determined on an Instron Table Model Universal

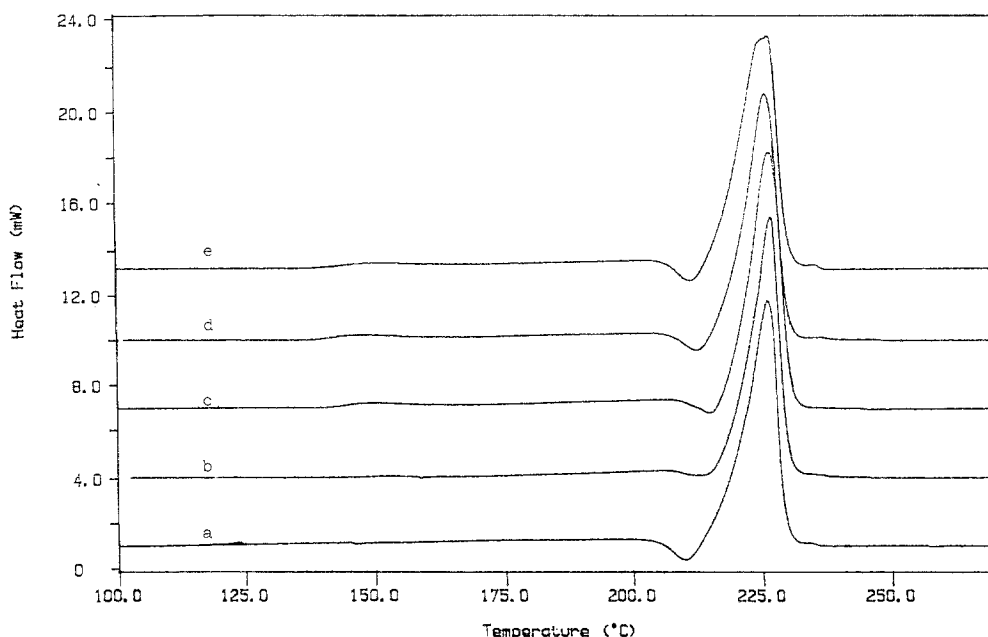


Figure 1 DSC thermograms: (a) quenched sample, and samples annealed at (b) 130°C for 4 h, (c) 8 h, d 16 h and (e) 32 h.

testing instrument (TM-S) at a temperature of about  $-110^{\circ}\text{C}$  and at a crosshead speed of  $5\text{ cm min}^{-1}$ . A minimum of four samples of each specimen type were tested and averaged. The standard deviation associated with each specimen was also calculated and shown in Table II.

Brown and Ward proposed a model which allows one to estimate the fraction of the interlamellar area covered by tie molecules ( $f_T$ )

$$f_T = (C\sigma_f - \beta E_{\text{iso}})/[\beta(E_T - E_{\text{iso}})] \quad (3)$$

where  $C$  represents the stress concentration,  $\beta$  is a constant of proportionality,  $E_{\text{iso}}$  the Young's modulus for van der Waals' bonds, and  $E_T$  the Young's modulus of the tie chains. For comparison purposes we used  $C = 50$ ,  $\beta = 0.1$ ,  $E_{\text{iso}} = 8\text{ GPa}$ ,  $E_T = 300\text{ GPa}$  as proposed by Brown and Ward for polyethylene.

### 2.3.5. Fracture surface morphology

Fatigue fracture surfaces were examined using an ISI-SX-40 scanning electron microscope. Prior to SEM examination, specimens were coated by a vacuum evaporated layer of gold for about 20 sec at 12 mA.

TABLE I Degree of crystallinity and second melting peak temperatures for the quenched and annealed samples

Sample	$W_c$ (%)	$T_m$ ( $^{\circ}\text{C}$ )
Quenched	40	221.3
A130 4 h	40	221.6
A130 8 h	40	221.5
A130 16 h	42	221.5
A130 32 h	42	221.7
A170 1 h	40	221.8
A170 2 h	40	221.8
A170 4 h	40	—
A170 24 h	42	221.7
A200 30 min	40	221.5
A200 1 h	42	221.8
A200 24 h	48	—

## 3. Results and discussion

### 3.1. Microstructural parameters

No significant change in degree of crystallinity, supermolecular structure or lamellar thickness was observed in the PBT samples for which we were able to observe stable fatigue crack growth. The DSC thermograms for the quenched and annealed samples are shown in Figs 1 to 3.  $W_c$  and the second melting peak temperature of the quenched and annealed specimens are summarized in Table I. Although difficult to detect in Fig. 1 due to the scale used, note that on scanning after annealing, an additional melting endotherm is observed at temperature between the annealing temperatures ( $T_a$ ) and the second melting temperature ( $\sim 221^{\circ}\text{C}$ ). In our recent investigation [15], the first melting endotherm, which has an onset temperature roughly a few degrees above the annealing temperature, has been shown to be associated with the crystals produced on annealing. For samples annealed at 170 and  $200^{\circ}\text{C}$ , heating rate experiments have shown that the second melting endotherm is at least partially associated with the melting of crystals formed by partial melting and recrystallization during scanning in the DSC. Nevertheless, the crystals formed during crystallization of the as-prepared quenched samples

TABLE II Summary of the intrinsic viscosities, molecular weights, brittle fracture strengths and evaluated tie chain densities.

Sample	$[\eta]$ ( $\text{dl g}^{-1}$ )	$M_n$	$\sigma_f$ (p.s.i.)	$f_T$ (%)
Quenched	0.735	20500	$9500 \pm 900$	8.3
A130 4 h	0.730	20300	$9000 \pm 800$	7.8
A130 8 h	0.690	18900	$7500 \pm 1000$	5.9
A130 16 h	0.617	16500	$6500 \pm 1000$	4.8
A130 32 h	0.578	15200	$6000 \pm 900$	4.2
A170 1 h	0.724	20000	$8600 \pm 1200$	7.3
A170 2 h	0.670	18200	$7200 \pm 1000$	5.7
A170 24 h	0.495	12600	$3200 \pm 400$	1.0
A200 30 min	0.663	18000	$7200 \pm 1200$	5.7
A200 24 h	0.472	11900	$2200 \pm 400$	—

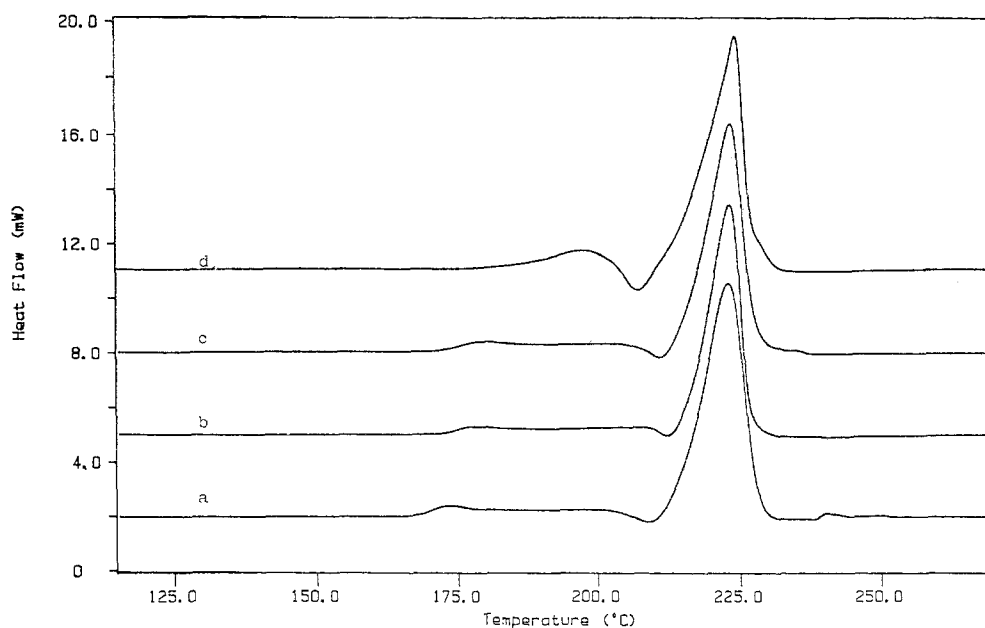


Figure 2 DSC thermograms: samples annealed at a 170°C for 1 h, b 2 h, c 4 h and d 24 h.

are believed to be associated with the second melting endotherm in the samples annealed at 200°C or lower. In addition, since the magnitude of peak 2 (reflecting the majority of the crystals, i.e., as-prepared crystals) is considerably larger than that of peak 1 for samples which we were able to observe stable crack growth, the second melting peak is, therefore, chosen as the  $T_m$  for evaluation of  $L$ . The estimated  $L$  for all these samples has a value of roughly 6.6 nm. Optical microscopy experiments show that all samples have the same type of supermolecular structure in which usual, unusual and, perhaps, "mixed" spherulites are included [16]. The average diameter of the supermolecular structure is roughly 10  $\mu\text{m}$ . SALS patterns were found to be circularly symmetric, presumably indicating a mixture of usual and unusual spherulites [17].

Table II summarizes the intrinsic viscosities, number average molecular weights calculated from Equation 2, the average brittle fracture strength ( $\sigma_f$ ) and the corresponding calculated tie chain density for the quen-

ched and annealed samples. Significant chain degradation was observed for most of the annealed samples except for samples annealed at 130°C for less than 4 h or at 170°C for less than 1 h. For example, annealing at 130°C for 32 h resulted in a reduction in  $M_n$  from about 20 000 to 15 000  $\text{g mol}^{-1}$ . The mechanism by which the degradation proceeds is not clear at this point. However, since  $W_c$  remains constant, it is reasonable to suppose that the degradation occurred preferentially in the amorphous phase. This suggestion explains the dramatic reduction in tie chain density as annealing time and temperature increases (see Table II).

### 3.2. Fatigue crack propagation

Fatigue crack propagation data of the quenched and annealing samples are shown in Fig. 4. The experimental errors associated with these runs are estimated and represented by two perpendicular error bars. It is interesting to note that the curves shift progressively

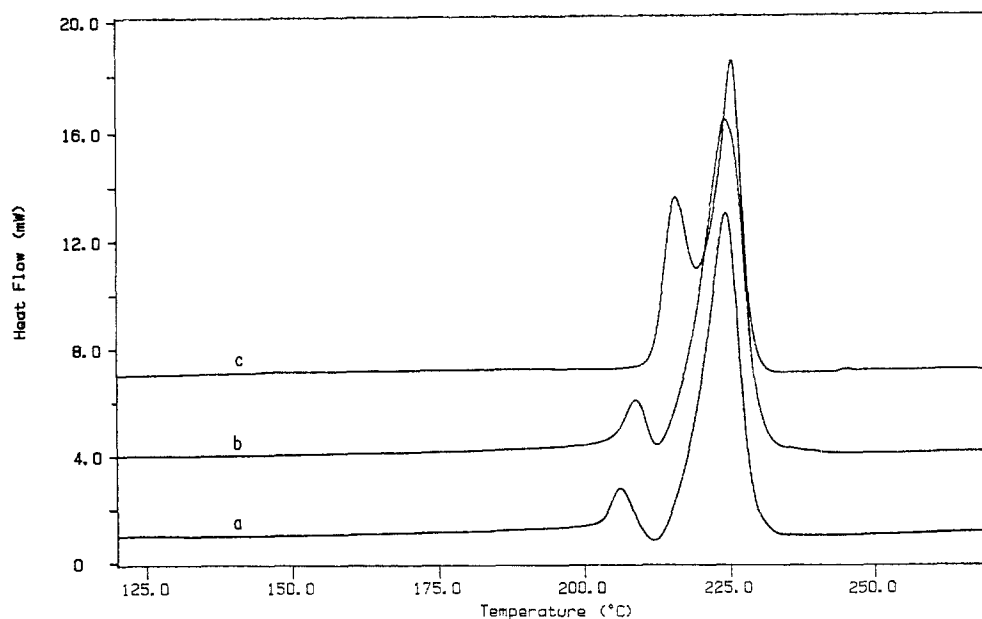


Figure 3 DSC thermograms: samples annealed at a 200°C for 30 min, b 1 h and c 24 h.

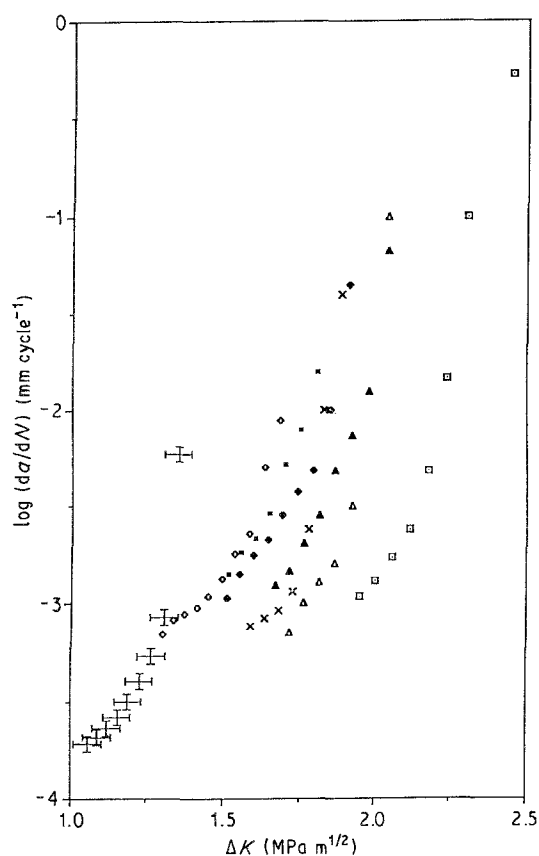


Figure 4  $da/dN$  plotted against  $\Delta K$  for the quenched and annealed samples. ( $\square$  quenched,  $\triangle$  A130 4h,  $\times$  A130 8h,  $\diamond$  A130 16h,  $+$  A130 32h,  $\blacktriangle$  A170 1h,  $\blacksquare$  A170 2h,  $\blacklozenge$  A200 30 min).

to lower  $\Delta K$  values with increasing annealing temperature and time. Consequently, some of the annealed samples are too brittle to obtain any stable crack growth data i.e. when annealing time is more than 4 h at 170°C or more than 1 h at 200°C. Since all of the other microstructural parameters, i.e.,  $W_c$ ,  $D$  and  $L$ , remained unchanged for samples exhibiting stable crack growth, it quickly became clear that the changes in FCP behaviour reflect the changes in  $M_n$  and  $f_T$ . For example, at a given  $\Delta K$  value, the FCP rate increases by about an order of magnitude as  $M_n$  decreases from 20 500 to about 16 500  $\text{g mol}^{-1}$  and  $f_T$  decreases from 8% to about 5%. No stable crack growth was observed when the tie chain density decreased to less than about 4% ( $M_n \sim 15\,000 \text{ g mol}^{-1}$ ). The influence of the tie molecule density has been isolated and found to exhibit a profound influence on the FCP behaviour of PBT.

### 3.3. Fracture surface analysis

Macroscopically, smooth fracture surfaces were observed for all the specimens. However, in the region of the slow crack growth, they display distinct features when viewed microscopically. An SEM micrograph of the fracture morphology of the quenched sample in the region of slow crack growth indicates the presence of many "voids" and drawn "ribbons" or "fibrils" (Fig. 5). These voids and drawn fibrils are likely to be remnants of a crazed damage zone which preceded the crack tip. Similar fatigue fracture surface morphologies have also been reported by Morelli and Takemori [18] for PBT. Let us focus on the micrographs (at a



Figure 5 Fracture surface of quenched sample in the region of slow crack growth.

somewhat lower magnification than in Fig. 5) of the slow crack growth region of the quenched sample and the series annealed at 130°C (Fig. 6). As the annealing time increases, there appears to be less plastic deformation and the length of the ribbons become shorter, characteristic of less ductile fracture. The micrographs of samples annealed at 170 and 200°C show a similar trend with increasing annealing time. The fracture surfaces associated with catastrophic failure of samples annealed for 24 h at both 170 and 200°C are relatively smooth without any observable drawn fibrils.

It is interesting to note that specimens with higher FCP resistance exhibit a rougher fracture surface, i.e. exhibit a greater degree of plastic deformation proceeding the propagating crack. These results can be reasonably explained by the idea that higher tie chain densities will lead to a more effective "entanglement" network in the crack tip region and result in a more highly deformable structure. As the tie chain density decreases below some critical value, the polymer becomes too weak to form a stable craze or similar structure in the crack tip region, and, therefore, no stable crack growth can be developed. This scenario is very similar to the mechanism proposed by Hertzberg and Manson [2], who suggested that the fatigue behaviour of semicrystalline polymers is determined at least partially by the stability of the entanglement network, i.e., by the tie chains linking the crystallites.

## 4. Conclusions

A significant decrease in FCP resistance was observed when PBT samples were annealed at different temperatures for various amounts of time. Morphological characterization shows that all the samples have the same percentage crystallinity, supermolecular structure and lamellae thickness but different number average molecular weight and calculated tie chain density. Chain degradation within the amorphous region during the annealing process is believed to be responsible for the decrease in both the average molecular weight and the tie chain density. SEM micrographs in the slow crack region indicate a clear transition to a more brittle like fracture surface when samples were annealed for longer time periods at a given annealing temperature. A decrease in tie chain density is suggested to be responsible for the significant change of the fracture

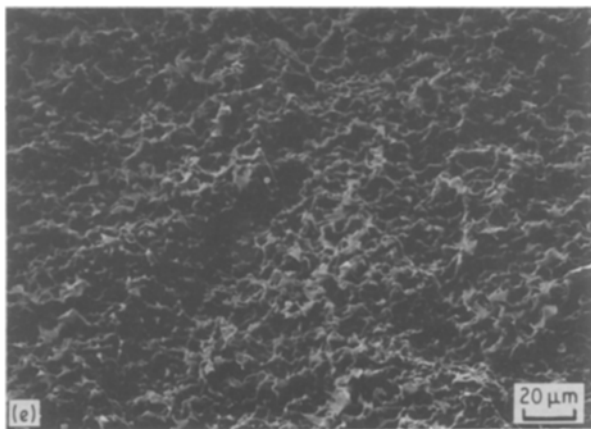
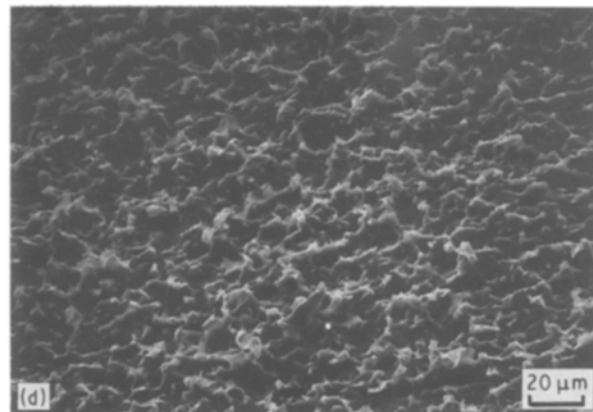
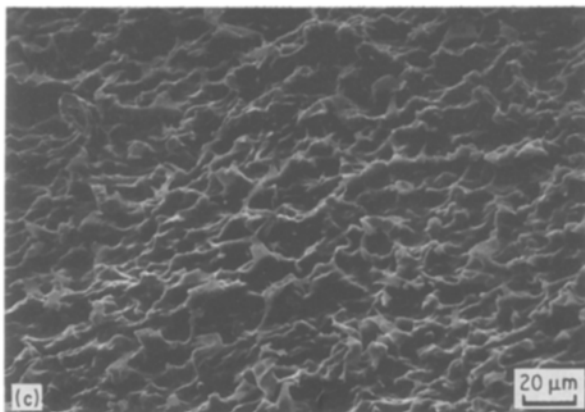
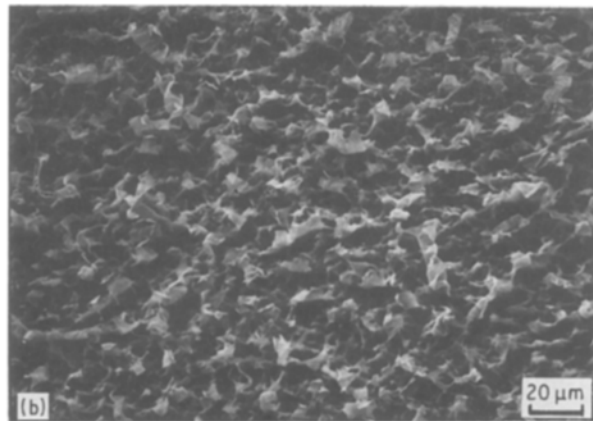
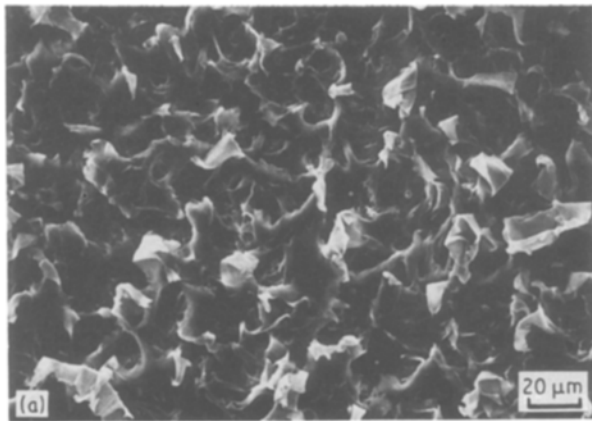


Figure 6 Fracture surfaces in the slow crack region for (a) quenched sample, (b) sample annealed at 130°C for 4 h, (c) 8 h, (d) 16 h and (e) 32 h.

surface and for the dramatic decrease in FCP resistance upon annealing.

### Acknowledgements

The authors would like to express their appreciation to the National Science Foundation (Grant DMR-8417554) for support of this work. Thanks is also extended to Dr Thomas Dolce of Hoechst Celanese for supplying the injection moulded PBT samples, to Ms Martine Jacq for consultation on the SEM work, and to Mr Frank Tallarico for preparing the dogbone specimens.

### References

1. R. W. HERTZBERG and J. A. MANSON, in "Fatigue of Engineering Plastics" (Academic Press, New York 1980).
2. J. A. MANSON and R. W. HERTZBERG, *Ency. Polym. Sci. Eng.* **7** (1986) 378.
3. F. X de CHARENTENAY, F. LAGHOUATI and J. DEWAS, in "Deformation, Yield and Fracture of Poly-

mers", (Plastics and Rubber Institute, London, UK, 1979), p.61.

4. A. RAMIREZ, J. A. MANSON and R. W. HERTZBERG, *Polym. Eng. Sci.* **22** (1982) 975.
5. K. FRIEDRICH, in "Proceedings of the 9th Conference on Scanning Electron Microscopy", (German Society for Testing Materials (DVM), Stuttgart, FRG, 1979) 173.
6. A. RAMIREZ, P. M. GAULTIER, J. A. MANSON and R. W. HERTZBERG, in "Fatigue in Polymers", (Plastics and Rubber Institute, London, UK, 1983) p. 31.
7. J. RUNT and M. JACQ, *J. Mater. Sci.* (1989) in press.
8. "1982 Annual Book of ASTM Standards", Part 10 (American Society for Testing and Materials, 1982) p. 765.
9. C. GOSTOLI, F. PILATI, G. SARTI and B. GIACOMO, *J. Appl. Polym. Sci.* **29** (1984) 2873.
10. J. DEVAUX, P. GODARD and J. P. MERCIER, *Makromol. Chem.* **179** (1978) 2201.
11. K. H. ILLERS, *Coll. Polym. Sci.* **258** (1980) 117.
12. J. D. HOFFMAN, G. T. DAVIS and J. I. LAURITZEN, in "Treatise on Solid State Chemistry", Vol. 3, edited by N. B. Hannay (Plenum Press, New York, 1975).
13. S. FAKIROV, N. AVRAMOVA and J. SCHULTZ, *Ang. Makromol. Chem.* **140** (1986) 63.
14. N. BROWN and I. M. WARD, *J. Mater. Sci.* **18** (1983) 1405.
15. J. T. YEH and J. RUNT, *J. Polym. Sci., Polym. Phys. Ed.* (1989) in press.
16. H.-J. LUDWIG and P. EYERER, *Polym. Eng. Sci.* **28** (1988) 143.
17. R. S. STEIN and A. MISRA, *J. Polym. Sci., Polym. Phys. Ed.* **18** (1980) 327.
18. T. A. MORELLI and M. T. TAKEMORI, *J. Mater. Sci.* **19** (1984) 385.

Received 27 May  
and accepted 12 September 1988